SYNTHESIS OF FUNCTIONALLY GRADED Al LM25/ZIRCONIA COMPOSITE AND ITS SLIDING WEAR CHARACTERIZATION USING RESPONSE SURFACE METHODOLOGY

N.Radhika[1]* and R.Raghu[2]

* n_radhika1@cb.amrita.edu

[1] Department of Mechanical Engineering, Amrita School of Engineering, Coimbatore Amrita Vishwa Vidyapeetham, Amrita University, India.
[2] Department of Metallurgical Engineering, PSG College of Technology, Coimbatore, India.

Abstract: *Functionally graded aluminium/zirconia metal matrix composite was fabricated using stir casting technique followed by horizontal centrifugal casting process and a hollow cylindrical functionally graded composite (150 x 150 x 16 mm) was obtained with centrifuging speed of 1200 rpm. The microstructural evaluation and hardness test was carried out on the outer and inner surface of the functionally graded composite at a distance of 1 and 13 mm from the outer periphery. In Response Surface Methodology, Central Composite Design was applied for designing the experiments and sliding wear test was conducted as per the design using a pin-on-disc tribometer for varying ranges of load, velocity and sliding distance. The model was constructed and its adequacy was checked with confirmation experiments and Analysis of Variance. The microstructural examination and hardness test revealed that the outer surface of FGM had higher hardness due to the presence of particle rich region and the inner surface had lesser hardness since it was a particle depleted region. The wear results showed that wear rate increased upon increase of load and decreased with increase in both velocity and sliding distance. Scanning Electron Microscopy analysis was done on the worn specimens to observe the wear mechanism. It was noted that wear transitioned from mild to severe on increase of load and the outer surface of FGM was found to have greater wear resistance at all conditions.*

1. INTRODUCTION

Aluminium Metal Matrix Composites (AMMCs) are materials used for numerous applications as they have superior mechanical and tribological properties. The incorporation of the reinforcement in the aluminium matrix enhances the strength, stiffness and wear resistance greatly, when compared to their monolithic alloy [1, 2]. Continuous research on these composites led to the development of Functionally Graded Material (FGM) which met the high performance requirement. FGM has continuous change in the microstructure, composition and properties in one direction [3, 4]. These multifunctional composites can be tailored towards specific applications used in automotive, aerospace, electronics and medical industries depending upon requirement [5].

The wide range of liquid state, solid state and deposition processes are available for the production of FGMs hence choosing the most

cost effective and simplest method is highly essential [6]. Centrifugal casting under liquid state processing was handled by researchers for successful production of the FGM [7], due to their advantages like greater control over the compositional gradient, cost effectiveness and better mold filling characteristics [8]. Microstructural examination of Functionally graded 6061/Silicon Carbide (SiC) Metal Matrix Composite (MMC) fabricated through centrifugal casting was carried out. The results revealed that outer periphery of the FGM had maximum reinforcement segregation and it decreased gradually towards inner periphery [9]. A numerical model was developed for the fabrication of functionally graded composite reinforced with diboride particles through centrifugal casting. It was reported that diboride particles were segregated at the outer region of the FGM and level of segregation depended upon rotation speed and centrifuging time [10]. Mechanical properties of functionally graded Al

356/SiC composite produced through centrifugal casting were investigated. It was found that high hardness of 140 HV was achieved at the outer periphery due to the presence of more particles and 90 HV was observed at the inner periphery due to particle depletion [11].

An assessment of the wear properties of the composites is highly necessary in order to make an impact on the development of tribo components in different fields. The wear behaviour of the composites was mostly investigated using statistical techniques to study the response under the influence of multiple variables and for the greater understanding of the process [12]. Dry sliding wear behaviour of Al-Cu-Mg/Titanium Dioxide (TiO_2) composite prepared by stir casting technique was studied using Taguchi's Design of Experiment (DOE) under the effect of parameters such as load, sliding speed and sliding distance. The result revealed that sliding wear behaviour was influenced by sliding distance followed by load and sliding speed whereas the frictional force was influenced by load followed by sliding speed and distance [13]. LM24 aluminium/SiC/Boron Carbide (B_4C) composite was developed with stir casting technique and its wear characteristics were investigated under the variation of parameters such as load (10, 20 and 30 N), speed (200, 300 and 400 rpm) and sliding distance (1000, 2000 and 3000 m) using Taguchi's technique. The wear behaviour was studied successfully through this technique and found out

that optimum condition to achieve the minimum wear rate was 10 N load, 400 rpm speed and 3000 m sliding distance [14].

From the literature exploration, it has been understood that wear behaviour of the FGM has not been revealed. Hence, the present investigation aims to deal with fabrication of functionally graded aluminum LM25/zirconia MMC using centrifugal casting technique and to investigate its mechanical properties as well as to study its dry sliding wear behaviour using Response Surface Methodology.

2. SELECTION OF MATERIALS

The LM25 aluminium alloy was selected as it has applications in automotive components like cylinder blocks and cylinder heads. The zirconia particles with 15 wt % and average size of 50 μm was preferred for reinforcing in the matrix and it has properties such as better hardness and greater wear resistance. The densities of the LM25 aluminium alloy and the zirconia particles were 2.68 g/cm³ and 5.68 g/cm³ respectively.

3. FABRICATION OF FGM

The FGM was produced using stir casting route followed by horizontal centrifugal casting technique. The LM25 aluminum alloy was taken in the graphite crucible and placed in the melting chamber of electric resistance furnace. Argon gas was supplied into this melting chamber during
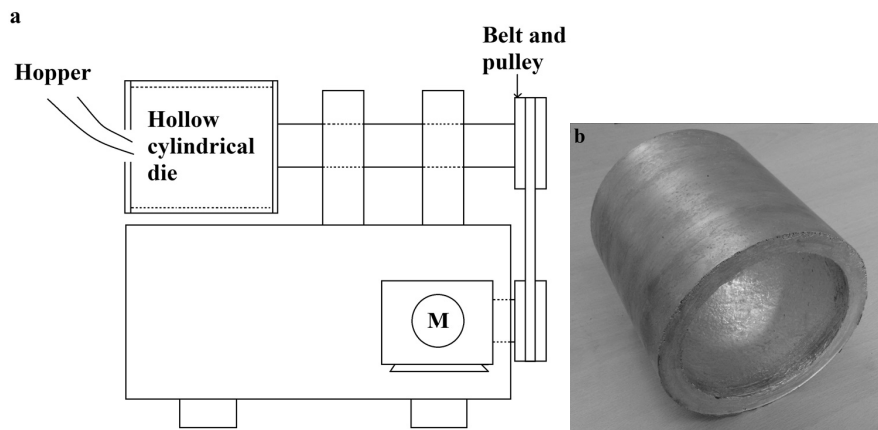

Fig. 1. a) Centrifugal casting setup and b) Hollow cylindrical FGM

melting of aluminium alloy in order to avoid the defects arising on the cast. Preheating of zirconia reinforcement particles was also done concurrently to remove the moisture content which helps to attain wettability with molten metal. Then the reinforcement particles were added to the molten metal through the hopper in the furnace. Stirrer setup equipped in the furnace was employed for stirring the molten metal with reinforcement particles at the speed of 200 rpm for 10 minutes. Creation of vortex during stirring allowed the reinforcement particles to suck into the molten metal which avoided floatation of the reinforcement particles. The hollow cylindrical die of the centrifugal casting setup (Figure 1a) was preheated simultaneously to avoid the temperature gradient between the molten metal and the die surface. The die was rotated at the speed of 1200 rpm and the molten metal was poured into the die and was allowed to solidified at room temperature. The obtained hollow cylindrical FGM has dimensions of 150 x 150 x 16 mm, which is shown in Figure 1b.

4. MICROSTRUCTURAL EXAMINATION

Specimens for microstructural analysis were taken at distances of 1 and 13 mm from outer periphery of the hollow cylindrical FGM. The specimens were polished initially with linisher polisher and then with the emery sheets of grades 1/0 and 2/0. Disc polisher was used for final polishing of specimens in order to attain fine surface. Etching on the specimen was done with Keller's reagent prior to examination under Zeiss Axiovert 25 CA Inverted Metallurgical Microscope.

The observed microstructures on the specimen's surface are shown in Figure 2a and 2b. The surface at distance of 1 mm (Figure 2a) has more reinforcement particles segregation and the surface at distance of 13 mm has less reinforcement particles (Figure 2b) which confirmed particles gradation occurred across the thickness of the hollow cylindrical FGM. The centrifugal force created during the centrifugal casting process was the reason for observing the compositional gradient and sharp transition between these two different surfaces. The centrifugal force acts on the molten metal containing the reinforcement particles enhances the high dense reinforcement particles to move away from the axis of rotation, where the same mechanism was observed [15]. The preheating of the hollow cylindrical die before pouring of the melt into the die decreased the temperature gradient between the molten metal and the die's inner surface. Therefore, it substantially reduced the solidification rate at the molten metal/die interface and the solidification front was avoided. Therefore, these particles acquired velocity under centrifugal force and gains time due to low solidification rate which causes the reinforcement particles to move towards the outer periphery thus forming the particle enriched zone at the distance of 1 mm. The surface at the distance of 13 mm from the outer periphery
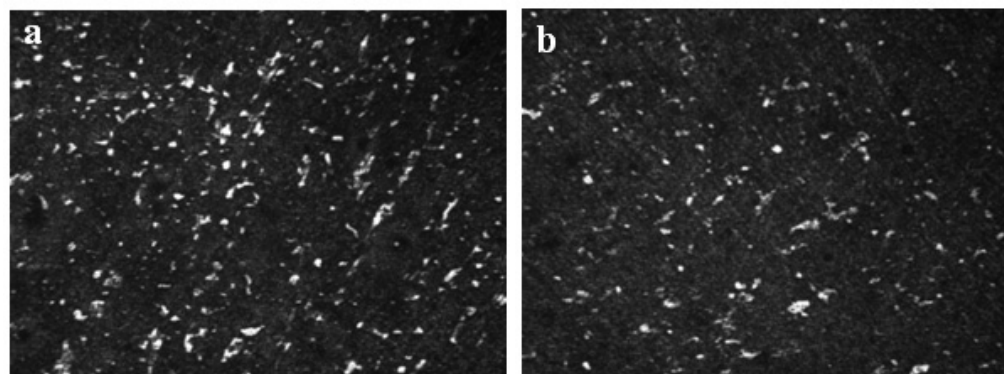

Fig. 2. Microstructure of the FGM a) Outer surface - 1 mm and b) Inner surface – 13 mm.

displayed fewer reinforcement particles with large matrix area as this was due to the movement of gas bubbles towards the inner periphery owing to their less density. These bubbles act as the carriers of the fewer reinforcement towards the inner periphery by obstructing the movement of reinforcement particles towards the outer periphery. The agglomerated particles with lesser density also get moved towards the inner periphery and the same characteristic was observed previously [16]. Thus, the functionally graded composite with graded distribution across the thickness of the casting with particle rich region at the outer periphery and particle depleted zone at the inner periphery was obtained by the centrifugal casting process.

5. HARDNESS TESTING

Surfaces at a distance of 1and 13 mm from the outer periphery were taken for hardness evaluation using Vicker's hardness tester. The specimens were polished using the emery sheets prior to test and the specimen was fixed over the base plate of the tester with the aid of holding jaws. The indenter made of diamond equipped in the tester was employed for producing indentation on the surface of specimen by applying a load of 100 gf load for 15 seconds. Automatic removal of the indenter from the specimen takes place and the diagonal length of the indentation was measured in order to obtain the hardness. Hardness values were measured five times on a surface and the final value was taken from its average. The obtained hardness for the surface at 1 mm and 13 mm from the outer periphery of FGM was 152 HV and 95 HV respectively which confirmed the particle gradient obtained across the thickness of the FGM. The surface at 1 mm displays higher hardness as this

surface has the particle enriched region which avoids the contact of the matrix with the indenter. This particle enriched zone strengthens the matrix zone and obstructs the deformation caused by the indenter due to the presence of hard reinforcement particles, a similar phenomenon was previously observed [17]. Thus, it avoids local deformation of the matrix and results in greater hardness. The surface at the distance of 13 mm displays less hardness as it has the particle depleted region with more matrix area. This softer matrix area was unable to obstruct the deformation hence large deformation takes place which leads to reduction in hardness. The results revealed that hardness was high at the outer periphery of the FGM and thus this surface was considered for dry sliding wear test since it is commonly known that the hardness is linearly related to the wear resistance.

6. RESPONSE SURFACE METHODOLOGY

Response Surface Methodology (RSM) is a statistical technique employed for studying response when influenced by many variables. This technique facilitates lesser experimental time and deep understanding of the response through the development of statistical model. This technique followed the procedure of: conducting experiments for different combination of parameters, prediction of regression coefficients through significance test, fitting of the experimental data, determining the response and checking adequacy of the fitted model. The applied load, velocity and sliding distance were the three parameters preferred and sliding wear rate was the selected response. To relate these parameters with the response, a second order polynomial model was developed and is given in the form of Eqn. (1)

Table 1. Wear parameters and their levels selected

Factors	Levels				
Load (N)	10	17	27	37	45
Velocity (m/s)	0.5	1.1	2.0	2.8	3.5
Sliding distance (m)	500	804	1250	1695	2000

$$Y_u = b + \Sigma b_i x_{iu} + \Sigma b_{ii} x^2_{iu} + \Sigma b_{ij} x_{iu}\, x_{ju} \qquad (1)$$

The response is Y_u and the coefficients are b, b_i, b_{ii}, and b_{ij}. The linear effect was determined by the second term, higher order effect was predicted by the third term and interaction's effect by the fourth term.

The selection of experiments and the analysis of the response were done through the statistical software Minitab 15. The Central Composite Design (CCD) under Response Surface Methodology was opted for planning the experiments and the number of parameters selected in this process elects the number of experiments. The wear process parameters such as load, velocity and sliding distance were varied for the range of 10-45 N, 0.5-3.5 m/s and 500-2000 m respectively (Table 1).

7. DRY SLIDING WEAR TESTING

The outer surface at the distance of 1 mm from the outer periphery of the hollow cylindrical FGM was subjected to dry sliding wear test in pin-on-disc tribometer at room temperature. The tribometer has the counter face steel disc of EN-32 with hardness of 60 HRC. The specimen holder was intended to hold the specimen and the loads were applied through the lever mechanism to keep continuous contact of specimen with the counter face. Track diameter for all the experimental runs was kept constant as 90 mm. Emery sheets were applied for removing the debris present over the steel disc in order to have fresh surface contact with the specimen. The experimental conditions designed using RSM was used for conducting the experimental runs. The specimen was measured for its mass prior to test and after completion of the wear test in order to calculate the wear rate.

8. RESULTS AND DISCUSSIONS

The experimental results obtained for the different combination of parameters generated as per CCD are shown in Table 2 and the results are further analyzed statistically.

The significance test was conducted to predict

Table 2. Experimental design and wear rate values obtained

S. No	Load (N)	Velocity (m/s)	Sliding distance (m)	Wear rate (mm^3/m)
1	27	2.0	1250	0.00189
2	27	2.0	1250	0.00185
3	37	2.8	1695	0.00231
4	27	0.5	1250	0.00227
5	37	2.8	804	0.00274
6	27	2.0	1250	0.00205
7	17	1.1	804	0.00184
8	10	2.0	1250	0.00102
9	27	2.0	500	0.00245
10	37	1.1	804	0.00306
11	17	2.8	804	0.00157
12	17	1.1	1695	0.00121
13	27	2.0	1250	0.00191
14	37	1.1	1695	0.00247
15	27	2.0	1250	0.00203
16	27	3.5	1250	0.00161
17	45	2.0	1250	0.00334
18	27	2.0	1250	0.00215
19	17	2.8	1695	0.00124
20	27	2.0	2000	0.00142

Table 3. Predicted regression coefficients for wear rate

Term	Coef	SE Coef	T	P
Constant	0.001943	0.000642	3.024	0.013
Load (N)	0.000030	0.000023	1.301	0.222
Velocity (m/s)	−0.000207	0.000254	−0.817	0.433
Sliding distance (m)	−0.000001	0.000001	−1.381	0.197
Load (N) * Load (N)	0.000001	0.000000	2.383	0.038
Velocity (m/s) * Velocity (m/s)	−0.000009	0.000041	−0.211	0.837
Sliding distance (m) * Sliding distance (m)	−0.000000	0.000000	−0.265	0.797
Load (N) * Velocity (m/s)	−0.000003	0.000005	−0.683	0.510
Load (N) * Sliding distance (m)	−0.000000	0.000000	−0.171	0.868
Velocity (m/s) * Sliding distance (m)	0.000000	0.000000	1.310	0.220

the regression coefficients and obtained coefficients are shown in Table 3. The acquired R2 and adjusted R2 from the significance test were 97.8 % and 95.8% respectively. These values were observed to be very nearer to each other which is evident that the model was adequate in relating the parameters with the response.

Using the regression coefficients from Table 3, the model constructed for evaluating the response is shown in Eqn. (2).

$$\text{Wear rate} = 0.001943 + 0.000030\,L - 0.000207V$$
$$-0.000001D + 0.000001L*L - 0.000009V*V$$
$$-0.000003L*V$$

$$(2)$$

where L is load (N), V is velocity (m/s), D is sliding distance (m).

From Eqn. (2) it was observed that response was influenced by the linear terms, square terms as well as interaction term. The term $L*V$ had high significance on the wear rate compared to other interaction terms such as $L*D$ and $V*D$. The parameter with the positive sign as coefficient in Eqn. (2) indicates that it had major impact on increasing the wear rate and parameter with the negative sign as coefficient indicated that it dominantly decreased wear rate. The model constructed using regression coefficients can be evaluated for its adequacy through the employment of confirmation experiments. The new value of the parameter was given as input in the constructed model and the response was evaluated. Wear experiments were conducted for these new set of values and the obtained experimental response and the model response were compared in order to estimate the error value (Table 4). The computed error percentage was observed to be below 5 % hence the model was found to be well adequate in valuing the sliding wear behaviour of the FGM by connecting with parameters such as load, velocity and sliding distance.

Table 4. Experimental and regression wear rates for new level of parameters

S.No	Load (N)	Velocity (m/s)	Sliding distance (m)	Experimental wear rate (mm³/m)	Regression wear rate (mm³/m)	Error (%)
1	12	0.8	700	0.00161	0.00154	4.34
2	19	1.5	1200	0.00131	0.00125	4.58
3	20	1.2	1300	0.00113	0.00110	2.65

Table 5. Analysis of Variance

| Source	DF	Seq SS	Adj SS	Adj MS	F	P
Regression	9	0.000007	0.000007	0.000001	49.18	0.000
Linear	3	0.000007	0.000000	0.000000	1.96	0.184
Square	3	0.000000	0.000000	0.000000	2.03	0.173
Interaction	3	0.000000	0.000000	0.000000	0.74	0.553
Residual Error	10	0.000000	0.000000	0.000000		
Lack-of-Fit	5	0.000000	0.000000	0.000000	1.33	0.381
Pure Error	5	0.000000	0.000000	0.000000		
Total	19	0.000007				

8. 1. Analysis of Variance

Analysis of Variance was made for 5 % significance level and for 95 % confidence level which determines the significance of the terms on the constructed model (Table 5). The regression model, coefficient model and lack of fit were evaluated for their significance through this analysis which gives the adequacy of the constructed model. It is known that standard value for 95 % confidence level is 5.05 hence the model would be adequate if the F value of lack of fit was less than this standard F value [18]. The acquired F value from the analysis was 1.33 which ensures that the developed model was good in relating the terms with the response and in prediction of the wear behaviour of the FGM.

8. 2. Influence of Parameters on the Sliding Wear rate

The experimental results obtained for the different parametric combinations were analyzed and the wear rate surface plots were generated for all combination of parameters which are shown in Figure 3-5. The effect of parameters on the wear rate has been detailed in the subsequent subsections.

8. 2. 1. Effect of Load on Sliding Wear of FGM

The surface plots for load with respect to velocity and sliding distance are shown in Figures 3 and 5 respectively. In both plots, the observed wear rate increased with increase in load and this was due to the linear increase in
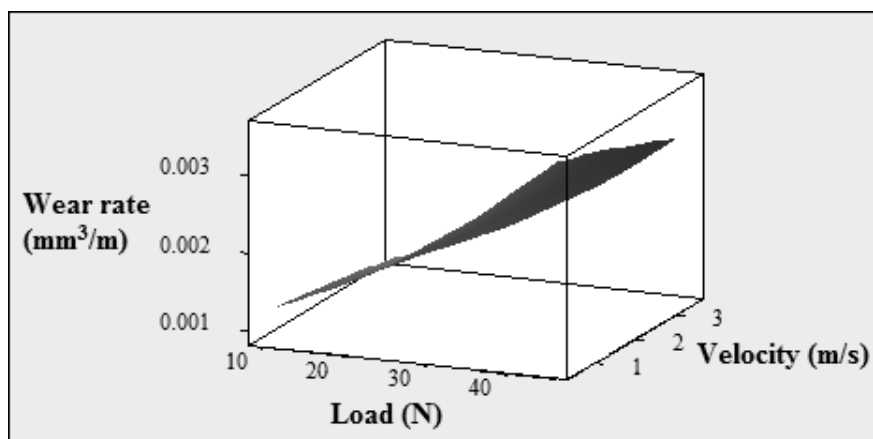
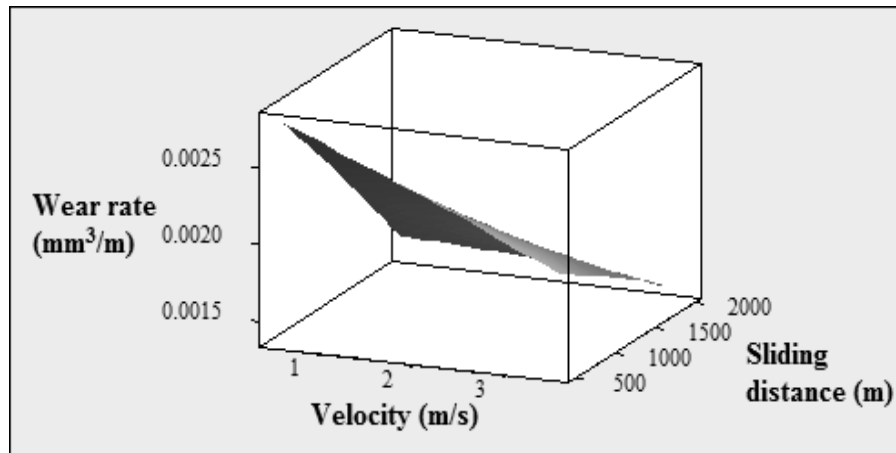**Fig. 3.** Wear trend for load and velocity at sliding distance of 1250 m.

Fig. 4. Wear trend for velocity and sliding distance at load of 27 N.

metallic contact of the specimen with the counter face of steel disc, a similar pattern was observed [19, 20]. The specimen exerted light pressure on the steel disc at low load which in turn resulted in very less amount of material removal from the surface of the specimen. When the load increased, the physical pressure at the interface increased and thereby material removal takes place in the form of debris. The debris in turn actively participate in removing more material from the specimen. The effect of high load makes the specimen to contact with steel disc at extreme pressure and deformation takes place which leads to high material removal.

8. 2. 2. Effect of Velocity on Sliding Wear of FGM

Wear trend surface plots for different levels of velocity with respect to load and sliding distance are represented in Figures 3 and 4 respectively. Wear rate was found to decrease with increase in velocity for a combination of both parameters as this was attributed to contact time of the interfaces. The specimen contacts the counter face at low velocities and the surface contact was observed to be high at this condition which results in high wear rate. On gradual increase of velocity, the wear rate decreases as the temperature between the contact surfaces gets increased. Oxidation of the material takes place which causes the materials to get transferred between the surfaces and results in forming oxide

layer called Mechanically Mixed Layer (MML). This hard MML protects the surface of the specimen from sliding wear hence the wear rate gets reduced and analogous behaviour was observed [21]. This layer protects and aids in less surface contact at high velocities and offers greater resistance to the sliding wear.

8. 2. 3. Effect of Sliding Distance on Sliding Wear of FGM

Wear surface plots for variation of sliding distance corresponding to load and velocity are represented in Figures 4 and 5 respectively. The increase of sliding distance led to decrease of wear rate in both situations. The specimen machined out of the hollow cylindrical FGM initially has fine surface and it gets into contact with the counter face during initial sliding. Thus the matrix surface eventually gets removed from the surface of the specimen and high wear rate was observed. Increase of sliding distance caused the hard reinforcement particles present in the surface of the composite specimen to get protruded after the removal of matrix area and acted as obstacles to sliding wear. Thus, the wear rate was found to be high at initial sliding distance and gets decreased when reaching greater distances.
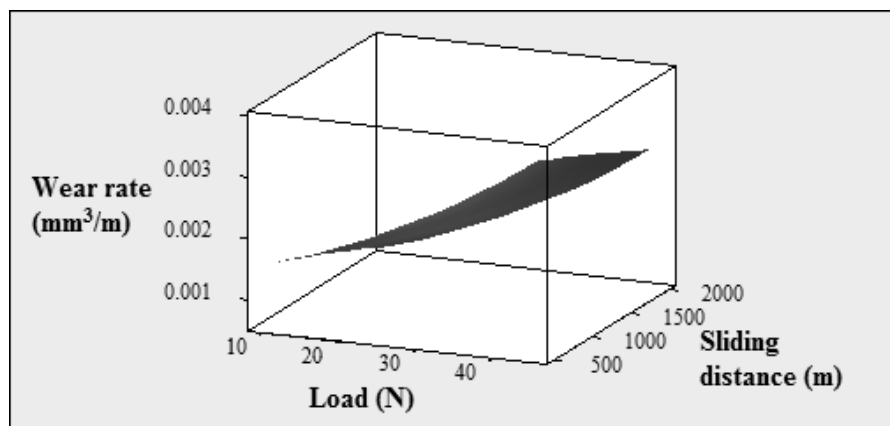
48

Fig. 5. Wear trend for load and sliding distance at velocity of 2 m/s.

8. 3. Response Optimization

The RSM optimizer in Minitab software was used for optimization process and to find out the global solution for achieving minimum wear rate. The objective of this investigation is to obtain minimum wear rate. Hence, the upper limit and target of wear rate were fed as inputs into the RSM optimizer. The optimum parametric solution obtained from the process to acquire minimum wear rate was at a load of 10 N, velocity of 0.6 m/s and sliding distance of 500 m.

9. SCANNING ELECTRON MICROSCOPY ANALYSIS

The surfaces worn at different parametric combinations were observed through Scanning Electron Microscope and are shown in Figure 6 a-d. The surfaces subjected to different load conditions (Figure 6a-c) were observed to recognize the effect of load on sliding wear mechanisms. The low load (10 N) worn surface (Figure 6a) indicated the presence of grooves at fewer places as this was reasoned to the less pressure acted on the surface of the steel disc by the specimen. On increase of load to 27 N on the surface (Figure 6b), continuous grooves were observed on the specimen surface with rise in material removal. The material removed as debris gets into contact at counter face/specimen

interface and trapping of the debris between the contacting surfaces made them to slide on the specimen surface due to continuous rotation of the steel disc. Thus it resulted in producing continuous grooves on the surface till it detaches from the specimen. The surface worn at high load (Figure 6c) revealed greater deformation with high material removal. The specimen contacts the disc with greater pressure at this load condition, hence the delamination with wide grooves was observed. Thus, the worn surface at different loads revealed that wear mechanism transitioned from mild to severe which confirmed the increase of wear rate on increase of load. Although the wear rate gets increase of load, the particle enriched outer surface of the FGM hindered the quick transition of wear from mild to severe. The zirconia reinforcement particles were extremely hard which obstructed deformation by reducing the contact of matrix with counter face and consequently it resulted in less material removal. The underlying mechanism for exhibiting greater wear resistance was the Orowan dispersion strengthening mechanism offered by the zirconia particles. The zirconia particles acted as the obstacles to dislocation motion. Therefore dislocation bends between these zirconia particles forming loop around the particles and moved forward. The loops were continuously formed over the particles by the movement of consecutive dislocations which created a back
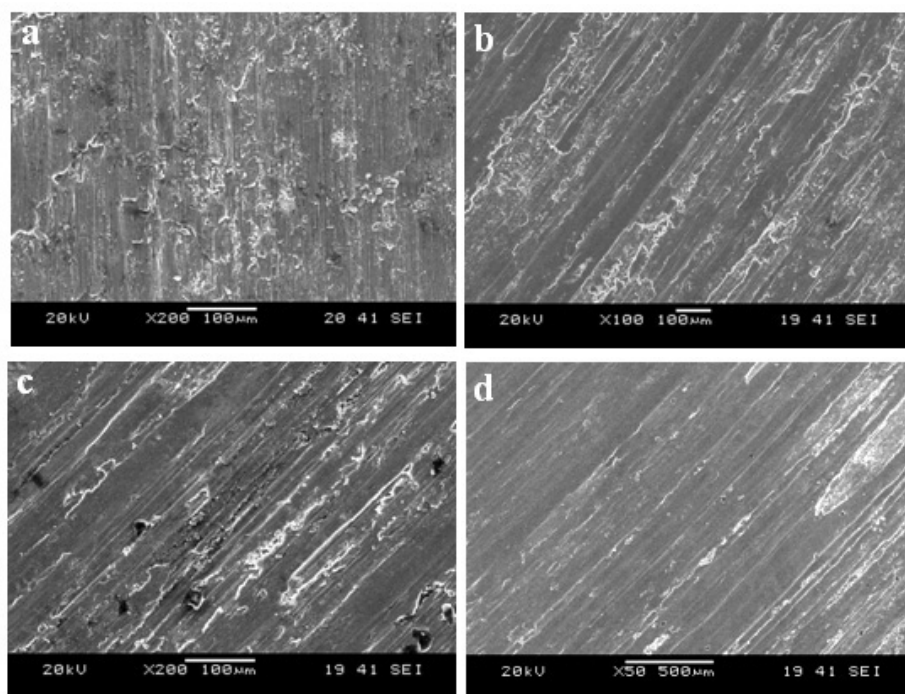
Fig. 6. SEM examination on worn surfaces a) L = 10 N, V = 2 m/s and D=1250 m, b) L = 27 N, V = 2 m/s and D = 1250 m, c) L = 45 N, V = 2 m/s and D = 1250 m and d) L = 27 N, V = 3.5 m/s and D = 1250 m.

stress which in turn restricted further dislocation movement. Therefore higher stress was essential for further slip process to take place which resulted in strengthening of the material [22- 24]. The necessary stress to overcome the back stress was inversely proportional to the inter-particle distance. This revealed that surface at the distance of 1 mm with more reinforcement concentration had less inter-particle spacing which exhibited greater wear resistance at all loads. Therefore, it is understood that zirconia reinforcement particles acted as the load bearing elements and significantly reduced the level of wear at all conditions.

To understand the wear mechanisms during transition of velocity, worn surface at high velocity (Figure 6d) was compared with the surface worn at low velocity with a similar load and sliding distance (Figure 6b). The high velocity action on the surface creates an increase in temperature at the interface and thereby material transfer takes place which led to formation of oxide layer over the surface of the specimen. This layer protects the specimen from wear hence better wear resistance was achieved. Thus, this surface resembles with less material removal compared to the surface worn at low velocity hence it was ensured that the increase in velocity decreased the wear rate on the specimen surfaces.

The surface worn at optimum condition (Figure 7) was considered for observing the wear
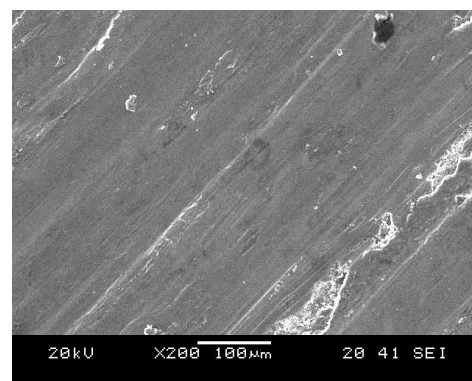

Fig. 7. Surface at optimum parametric condition

mechanisms through SEM to check the adequacy of the model. This surface revealed shallow, fine grooves and scratches indicating minimum removal of material which ensures that the model relates the wear process parameters with the response for predicting wear behaviour.

10. CONCLUSION

Functionally graded aluminium/zirconia metal matrix composite was successfully produced through stir casting followed by horizontal centrifugal casting technique. The microstructural characterization shows that particle rich region was formed at outer periphery and the particle depleted region was formed at inner periphery under centrifuging effect. High hardness of 152 HV was obtained at outer periphery and low hardness of 95 HV was obtained at the inner periphery. The wear model has been constructed successfully and was found to be adequate with confirmation experiments and Analysis of Variance. Wear plots showed that wear trend increased with increase in load and decreased with increase in velocity and sliding distance. The optimum condition to acquire the minimum wear rate was at a load of 10 N, velocity of 0.6 m/s and at a sliding distance of 500 m. The Scanning Electron Microscopy examination revealed that load had the effect of changing the wear from mild to severe and the reinforcement particles present in the outer surface of the composite enhanced the wear resistance by delaying the transition of wear. Therefore, this functionally graded composite can be used for the development of applications like brake drum, cylinder liners and cylinder blocks, and can be used in situations where high wear resistance is a necessity.

REFERENCES

1.   Vijaya Ramnath, B., Elanchezhian, C., Annamalai, R. M., Aravind, S., Sri Ananda Atreya, T., Vignesh, V. and Subramanian, C., "Aluminium Metal Matrix-A Review". Rev. Adv. Mater. Sci., 2014, 38, 55-60.
2.   Radhika, N., Subramanian, N. and Venkat Prasat, S., "Wear Behaviour of Aluminium/Alumina/Graphite Hybrid Metal Matrix Composite Using Taguchi's Techniques". Ind. Lubr. Tribol., 2013, 65, 166-174.
3.   Navneet, S., Hitesh, U., Retaish, U. and Karamjeet, S., "FGM Rotating Disc Fabricate by Al/Al$_2$O$_3$." Int. J. of Eng. Appl. Sci. Res., 2012, 1, 33-37.
4.   Radhika, N. and Raghu, R., "Experimental Investigation on Abrasive Wear Behaviour of Functionally Graded Aluminium Composite". J. Tribol., 2015, 137, 1-7.
5.   Kumar, R. and Chandrappa, C. N., "Synthesis and Characterization of Al-SiC Functionally Graded Material Composites Using Powder Metallurgy Techniques". Int. J. of Innovative Res. Sci. Eng. Technol., 2014, 3, 15464-15471.
6.   Rajan, T. P. D. and Pai, B. C., "Development in Manufacturing Processes of Functionally Graded Materials". Int. J. Adv. Eng. Appln., 2009, 2, 64-74.
7.   Ferreira, S. C., Velhinho, A., Rocha, L. A. and Braz, F. M., "Microstructure Characterization of Aluminium Syntactic Functionally Graded Composites Containing Hollow Ceramic Microspheres Manufactured by Radial Centrifugal Casting". Mater. Sci. Forum, 2008, 587, 207-211.
8.   Radhika, N and Raghu, R., "Development of functionally graded aluminium composites using centrifugal casting and influence of reinforcements on mechanical and wear properties". Trans. Nonferrous Met. Soc., 2016, 26, 905-916.
9.   Vinoth Babu, K., Rajan, T. P. D., Pillai, R, M. and Pai, P. C., "Fabrication of Functionally Graded Aluminium Metal Matrix Composites and its Mechanical Behaviour Using Artifical Neural Network". Int. J. Adv. Eng. Appln., 2009, 2, 21-27.
10. Gutierrez, G., Suarez, M. O. and Giordano, M. A., "Numerical Modeling of Centrifugal Casting of Functionally-Graded Aluminium Matrix Composites Reinforced with Diboride Particles". Mecanica Computacional., 2007, 26, 2612-2622.
11. Jayakumar, A. and Rangaraj, M., "Property Analysis of Aluminium (LM-25) Metal Matrix Composite". Int. J. Emerg. Technol. Adv. Eng.,

2014, 4, 495-501.

12. Kr.Mishra, A., Sheokand, R. and Srivastava, R. K., "Tribological Behaviour of Al-6061/SiC Metal Matrix Composite by Taguchi's Techniques". Int. J. Sci. Res. Publ., 2012, 10, 1-8.

13. Hemanth Kumar, T. R., Swamy, R. P. and Chandrashekar, T. K., "Taguchi Technique for the Simultaneous Optimization of Tribological Parameters in Metal Matrix Composite". J. Miner. Mater. Charact. Eng., 2011, 10, 179-188.

14. Uvaraja, V. C. and Natarajan, N., "Optimization on Friction and Wear Process Parameters Using Taguchi Technique". Int. J. Eng. Technol., 2012, 2, 694-699.

15. Shivaji, V. Gawali and Vinod B. Tungikar., "Study of Behavioral Pattern in Wear Applications Composite in Presence of Different Geometric Shapes". Sastech J., 2013, 12, 15-19.

16. Kai, W., Han-Song, X., Mao-Hua, Z. and Chang-Ming, L., "Microstructural Characteristics and Properties in Centrifugal Casting of SiCp/Z1104 composite". Trans. Nonferrous Met. Soc. China, 2009, 19, 1410-1415.

17. Savas, O., Kayikci, R., Ficici, F. and Koksal, S., "Production of Functionally Graded AlB_2/Al-4%Mg Composite by Centrifugal Casting". Period. Eng. Nat. Sci., 2013, 1(2), 38-43.

18. Niranjan, K. and Lakshminarayanan, P. R., "Optimization of Process Parameters for In Situ Casting of Al/TiB_2 Composites through Response Surface Methodology". Trans. Nonferrous Met. Soc. China, 2013, 23, 1269-1274.

19. Singla, M., Singh, L. and Chawla, V., "Study of Wear Properties of Al-SiC Composites". J. Miner. Mater. Charact. Eng., 2009, 8 (10), 813-821.

20. Radhika, N., Subramanian, R., Venkat prasat, S. and Anandavel, B., "Dry Sliding Wear Behaviour of Aluminium/Alumina/Graphite Hybrid Metal Matrix Composites". J. Ind. Lubr. Tribol., 2012, 64, 359-366.

21. Veeresh Kumar, G. B., Rao, C. S. P. and Selvaraj, N., "Mechanical and Tribological Behavior of Particulate Reinforced Aluminum Metal Matrix Composites – a review". J. Miner.

Mater. Charact. Eng., 2011, 10, 59-91.

22. Yuvaraj, N., Aravindan, S. and Vipin, "Fabrication of Al5083/B_4C Surface Composite by Friction Stir Processing and its Tribological Characterization". J. Mater. Res. Technol., 2015, 4, 398-410.

23. Mazahery, A. and Shabani, M. O., "Characterization of Cast A356 Alloy Reinforced with NanoSiC Composites". Trans. Nonferrous Met. Soc. China., 2012, 22, 275-280.

24. Casati, R. and Vedani, M., "Metal Matrix Composites Reinforced by Nano-particles-A Review". Metals, 2014, 4, 65-83.